

## Original Article

# Circ5379-6, a circular form of tumor suppressor *PPARα*, participates in the inhibition of hepatocellular carcinoma tumorigenesis and metastasis

Ning Zhang<sup>1\*</sup>, Guohua Li<sup>2\*</sup>, Xiaoxing Li<sup>3</sup>, Lixia Xu<sup>1</sup>, Minhu Chen<sup>1</sup>

<sup>1</sup>Department of Gastroenterology, The First Affiliated Hospital, Sun Yat-sen University, Guangzhou 510080, China;

<sup>2</sup>Department of Gastroenterology, Shunde People's Hospital, Nanfang Medical University, Foshan 528300, China;

<sup>3</sup>State Key Laboratory of Oncology in South China, Collaborative Innovation Center for Cancer Medicine, Sun Yat-sen University Cancer Center, Guangzhou 510080, China. \*Equal contributors.

Received May 9, 2018; Accepted October 25, 2018; Epub November 15, 2018; Published November 30, 2018

**Abstract:** This study aimed to investigate the role of circRNAs encoded by *PPARα* in regulating the pathogenesis processes of hepatocellular carcinoma (HCC). Comprehensive analysis of 3 circular RNA databases revealed multiple circular RNAs within the *PPARα* gene. The candidate circRNAs were first structurally validated via specific convergent and divergent primer amplification, RNase R treatment, and Sanger sequencing. According to a further validation of the cell viability assay, cell cycle and apoptosis, and transwell assays, the circRNAs correlated to *PPARα* were obtained. Their functions in tumorigenesis were further validated via the subcutaneous tumor model and the migration model in nude mice. We showed that the overexpression of circ5379-6 decreased cell proliferation, inhibited cell migration and invasion, and induced cell apoptosis in the HCC cell lines. Consistently, *in vivo* studies in nude mice confirmed that the overexpression of circ5379-6 effectively inhibited the tumorigenesis and metastasis of HCC. We conclude that circ5379-6 plays a role similar to its linear counterpart *PPARα* to inhibit HCC tumorigenesis and progression.

**Keywords:** Hepatocellular carcinoma, circular RNA, *PPARα*, tumorigenesis, metastasis

## Introduction

Hepatocellular carcinoma (HCC) is the fifth most common cancer and the third leading cause of cancer related death in the world [1]. There are an average of 700,000 cases of HCC each year, with 600,000 attributable deaths [2]. Among these cases, around 75% occur in Asia and the Pacific Islands, while China accounts for 55% of HCC cases worldwide [3, 4]. It is therefore important to identify the risk factors in order to further develop an understanding of the molecular and cellular processes involved, and thereby refine the search for new therapeutic and molecular targets.

Circular RNAs (circRNAs) are RNA molecules with a loop structure generated from the aberrant splicing of the transcripts [5]. Their expression has been discovered across different species, thanks to the development of the next-generation sequencing [6]. The correlation be-

tween the levels of circRNAs and their corresponding linear mRNA is not clear, but it appears that at least some circRNAs are positively correlated to the level of their linear isoforms [7]. Compared with linear RNA, circRNA are resistant to RNase R, and can be stable in cells, exhibiting half-lives of >48 h [8, 9]. Therefore, circRNAs are not simply by-products, but should be involved in biological processes.

Recently, circRNAs have emerged as having potential involvement in the regulation of tumor biology and function through molecular mechanisms [10, 11]. One has been shown to be a potential novel biomarker for hepatocellular carcinoma [12], but the function of circRNAs in HCC is not comprehensively understood. In another case, the differential expression of multiple circRNAs in HCC tissues and their clinical significance in hepatitis B-related HCC patients was revealed [13]. CircRNAs undeniably perform functions in regulating HCC. For

instance, circRNA expression is suppressed by androgen receptor-regulated adenosine deaminase, thereby regulating HCC proliferation [14]. However, their function in the pathology of HCC remains to be investigated.

Peroxisome proliferator-activated receptors (PPARs) are ligand-activated nuclear receptors belonging to the steroid/thyroid hormone receptor superfamily [15]. Among the PPARs, PPAR $\alpha$  regulates the constitutive transcription of genes encoding fatty-acid-metabolizing enzymes and is associated with the maintenance of fatty acid transport and metabolism [16]. From the existing studies, long-term administration of PPAR $\alpha$  ligands to rodents causes accelerated hepatocyte proliferation, increased ROS generation, and increased development of HCC [17, 18]. In this case, the inhibition of the expression of PPAR $\alpha$  benefits the individual to protect against HCC development [19]. Our previous study suggested that PPAR $\alpha$  deficiency enhances susceptibility to DEN-initiated HCC and that PPAR $\alpha$  suppresses tumor cell growth through inhibiting cell proliferation and inducing cell apoptosis via direct targeting of the I $\kappa$ B $\alpha$  and NF- $\kappa$ B signaling pathway [20]. This evidence suggests that PPAR $\alpha$  is an important gene in liver tumorigenesis.

CircRNAs have been suggested to share some functions with their linear counterparts [21]. Previously, we indicated the role of PPAR $\alpha$  in hepatocarcinogenesis. Here, we investigated whether or not the circular form of PPAR $\alpha$  also exerts its effect on HCC growth and metastasis.

## Materials and methods

### Cell culture

The hepG2, 293T, Huh-7, and SK-hep-1 cell lines were obtained from ATCC (Manassas, VA, USA). The cell lines were maintained in a humidified chamber with 5% CO<sub>2</sub> in low-glucose DMEM culture medium containing 10% FBS, 100 U/ml penicillin, and 100  $\mu$ g/ml streptomycin. For subculturing purposes, cells were detached by 0.05% trypsin-EDTA treatment at 37°C.

### CircRNA validation and RT-PCR

Total RNA was purified from cells with TRIZOL reagent (Invitrogen, USA), following the ma-

nufacturer's instructions. RNA (with/without RNase R treatment) was then reverse transcribed using the GoScript RT system (Promega, Madison, WI, USA). CircRNA was validated via PCR, using divergent and convergent primers and gDNA was used as the control. In order to quantify circRNA and mRNA, real-time PCR (qPCR) was performed with GoTaq qPCR Mastermix in ABI 7500 fast system (Applied Biosystem, USA). Sanger sequencing of all PCR products was performed for validation of the circRNA.

### Overexpression of circRNA

Full-length targeted circRNAs were amplified by PCR using primers directly flanking the head-to-tail splice sites. The full-length circRNA, along with an 800 bp flanking sequence upstream of the splice acceptor, was cloned into the lentiviral expression vector pLVX-IRES-neo (Clontech Laboratories, San Francisco, CA, USA) according to the manufacturer's instructions. The upstream flanking sequence was inserted downstream in the reverse orientation. The constructed vector was verified by Sanger sequencing. The vectors were thereby transfected into cell lines using lipofectamine 2000 (Thermo Fisher, USA), according to the manufacturer's instructions. The expression levels of the circRNA and targeted mRNAs were determined with qPCR.

### Cell viability assay

Cells were seeded at a density of  $2 \times 10^4$  cells/well in a 96-well plate and cultured for 3 days in DMEM medium with 10% fetal bovine serum (FBS) and antibiotics. Cell viability was examined with the CellTiter96Aqueous One Solution Cell Proliferation Assay (MTS, Promega, Poland). MTS solution was diluted 10 $\times$  in DMEM and 400  $\mu$ l aliquots were added per well. The absorbance at 490nm was measured after 30 min incubation at 37°C in the dark.

### Colony formation assay

Cells (100, 200, or 400) were seeded into 6-well plates, and incubated at 37°C and 5% CO<sub>2</sub> for 14 days. They were then fixed in methanol for 15 min, stained with 0.05% crystal violet, and were counted.

## *Migration and invasion assays*

A 24-well plate containing 8 mm-pore size chamber inserts (Corning, USA) was used to evaluate the migration and invasion of tumor cells. For the migration assay,  $1 \times 10^5$  cells were seeded in the upper chamber. For the invasion assay, the membrane was coated with Matrigel (BD Biosciences, USA) to form a matrix barrier, whereupon  $2 \times 10^5$  cells were placed in the upper chamber. In each lower chamber, 600  $\mu$ l of DMEM medium with 10% FBS was added. Cells were incubated at 37°C and allowed to migrate for 36 h or invade for 48 h. After incubation, the cells that had migrated through the pore were fixed with 4% paraformaldehyde and stained with 0.1% crystal violet. Next, the cells were counted and photographed under an IX71 inverted microscope (Olympus, Tokyo, Japan).

## *Cell cycle apoptosis assay*

Cells were seeded into 6-well plates,  $5 \times 10^5$  per well and allowed to adhere overnight at 37°C. The cells were trypsinized, washed with PBS, fixed with 70% ethanol on ice, and resuspended in 500  $\mu$ l of propidium iodide solution for staining. The cell suspensions were assayed using a FACSCalibur flow cytometer (BD Biosciences, USA) at an excitation wavelength of 488 nm and an emission wavelength of 620 nm. The 10,000 gated events were collected by CellQuest Pro software (BD Biosciences), and flow cytometry data were analyzed with WinList and ModFit from Verity Software House (Topsham, USA). For the apoptosis assay, the cells were resuspended in 1 $\times$  binding buffer and 5  $\mu$ l of fluorochrome-conjugated Annexin V and 5  $\mu$ l of propidium iodide staining solution were added. The samples were tested using a FACSCalibur flow cytometer and the percentage of apoptotic cells was measured.

## *Immunohistochemical staining*

Paraffin-embedded tissue sections were given antibody thermal remediation, the activity of endogenous peroxidase was inhibited by hydrogen peroxide, and they were then blocked by serum after deparaffinization and hydration. The sections were incubated with 1:100 primary antibody overnight at 4°C, before being washed with PBS and incubated with the secondary antibody. The secondary antibody was then eliminated and the section was washed

again with PBS. DAB was applied for staining. The expression level of the molecules was estimated with microscopy.

## *HE staining*

The formalin fixated and paraffin embedded (FFPE) tissues were cut into sections and placed on slides, which were deparaffinated by xylene and washed with ethanol and water. Hematoxylin was applied for staining and the slides were washed with water for 10 minutes and ethanol for 5 s, stained with eosin, then incubated for 10 s. After incubation, the slides were washed again with water and cover-slipped. The slide images were obtained by microscopy.

## *In vivo experiments*

Male nude mice (Charles River Laboratories, Saint Constant, Canada) aged 6-8 weeks were housed in a pathogen-free environment. This animal experiment was approved by The Institute Research Medical Ethics Committee of Sun Yat-sen University.

For the subcutaneous tumor model,  $2 \times 10^6$  cells suspended in a final volume of 100  $\mu$ l were injected subcutaneously in the right flank of nude mice. The control was injected with saline. Tumor growth was measured every week using a dial caliper, with subcutaneous tumor volume calculated as  $(\text{length} \times \text{width}^2)/2$ . Animals were sacrificed after 5 weeks and the tumor was collected, fixed in formalin, and embedded in paraffin.

For the *in vivo* migration assay,  $2 \times 10^6$  cells suspended in a final volume of 100  $\mu$ l were injected in the tail vein. After 5 weeks, the mice were sacrificed, the lung tissue was collected, fixed in formalin, and embedded in paraffin. The FFPE sections were then used for HE staining.

## *Statistical analysis*

When data corresponded to a normal distribution, comparisons were performed using independent t-tests, one-way ANOVA, and two-way ANOVA. Non-parametric Mann-Whitney U, K-S, Kruskal-Wallis, and Wilcoxon tests were performed if data did not correspond to a normal distribution. The significance was established as  $P < 0.05$ . SPSS and GraphPad Prism software were used for the statistical analysis.

## hsa-circRNA5379-6

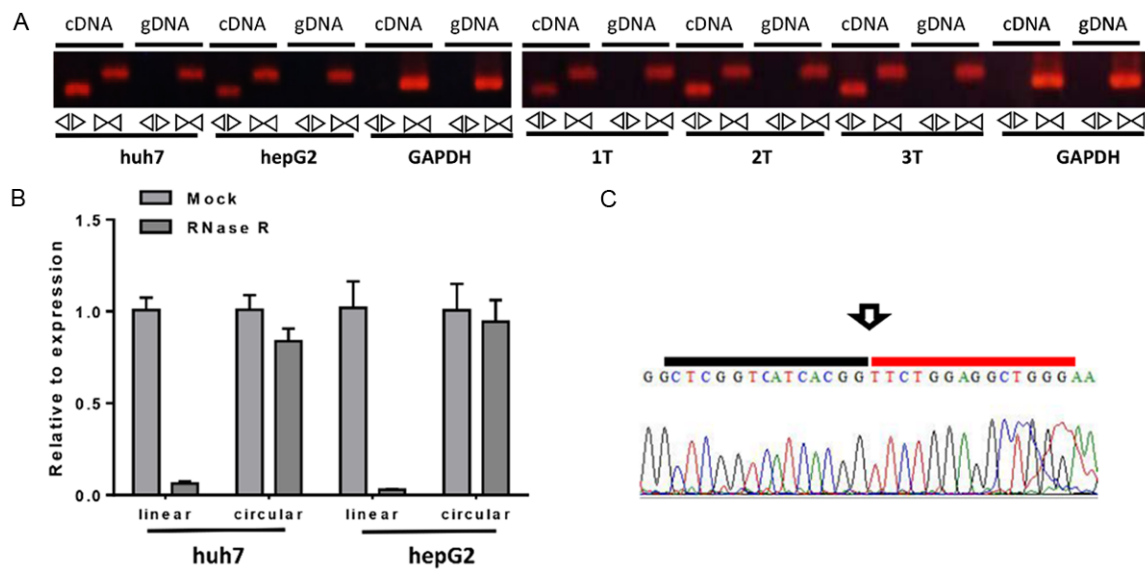


**Figure 1.** Verification the Cyclization sites and characterization of hsa-circRNA5379-6. A. The cDNA of circ5379-6 can be amplified by both divergent and convergent primers, but gDNA can be amplified only by convergent primers in the huh7 cell line, hepG2 cell line, and 3 cases of hepatocarcinoma (1T, 2T, and 3T) tissues. GAPDH was used as the linear control. B. RNase R was used to digest the linear RNA, the predicted circular RNA was resistant to RNase R treatment. C. Sanger sequencing depicts the junction of hsa-circRNA5379-6.

## Results

### Validation of circRNAs

RNA was purified from the huh7 cell line, hepG2 cell line, and hepatocarcinoma tissues for the purpose of screening the circRNAs. Comprehensive analysis of 3 circular RNA databases revealed multiple circular RNAs within the *PPARα* gene. Seven of these were validated to be expressed in huh7, hepG2, and hepatocarcinoma tissues, including circ0063781, circ0116792, circ0116794, circ0116795, circ0004706, circOverlap-8, and circ5379-6 (**Figures 1, S1, S2, S3, S4, S5 and S6**). For these validated circRNAs, the specific divergent primers could amplify PCR products with cDNA, but not with gDNA. However, the convergent primers could amplify PCR products successfully with cDNA and gDNA. RNase R was used to digest the linear RNA, and thereby the cDNA generated from mRNA could not be detected by qPCR, but qPCR worked for cDNAs generated from the circRNAs. In addition, the results of Sanger sequencing presented the junction sequences of the circRNAs to validate their presence in a circular structure. From the evidence provided by the experiments above, we continuously

screened candidate circRNAs correlated with hepatocellular carcinoma and verified their functions.

### Screening the candidate circRNAs involved in hepatocellular carcinoma

To study the potential roles of circ0063781, circ0116792, circ0116794, circ0116795, circ0004706, circOverlap-8, and circ5379-6 in HCC growth and metastasis, they were overexpressed in HepG2, Huh7, and Sk-hep-1 HCC cells. As shown in **Figure 2**, circ0063781, circ0116794, circ0116795, and circ5379-6 were successfully overexpressed in HepG2 and 293T cells, while we failed to detect circ0116792, circ0004706, and circOverlap-8 overexpression in either HepG2 or 293T cells (**Figure 2**). Thus, circ0063781, circ0116794, circ0116795, and circ5379-6 were selected for further analysis. The qPCR results confirmed that all these circRNAs except circ0063781 were upregulated in both Huh-7 and Sk-hep-1 cells (**Figure 3A-D**).

In order to identify the functions of circ0116794, circ0116795, and circ5379-6, an MTS assay was performed and showed that circ5379-6

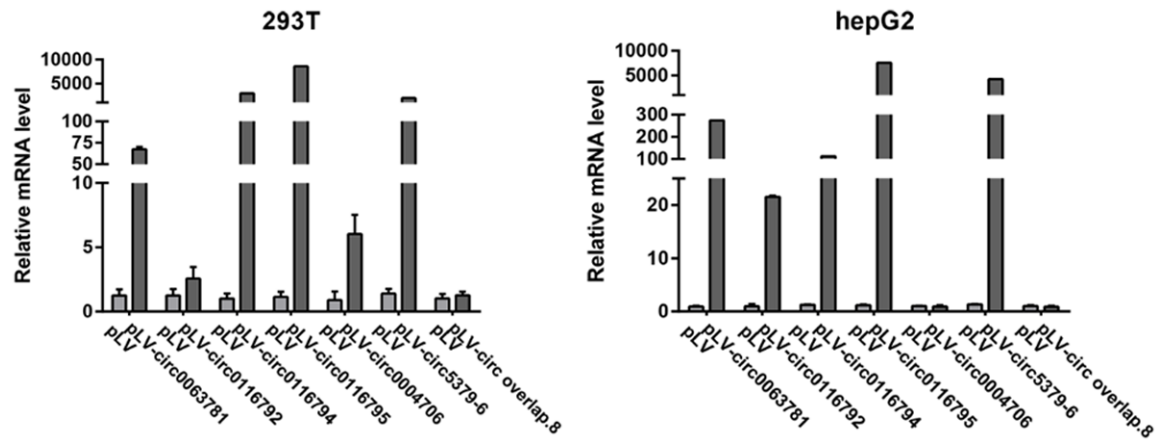


**Figure 2.** Overexpression of circRNAs in 293T and hepG2 cells. The performance of circ0063781, circ0116792, circ0116794, circ0116795, circ0004706, circ5379-6, and circ overlap-8 expression in 293T and hepG2 cells was verified by qPCR.

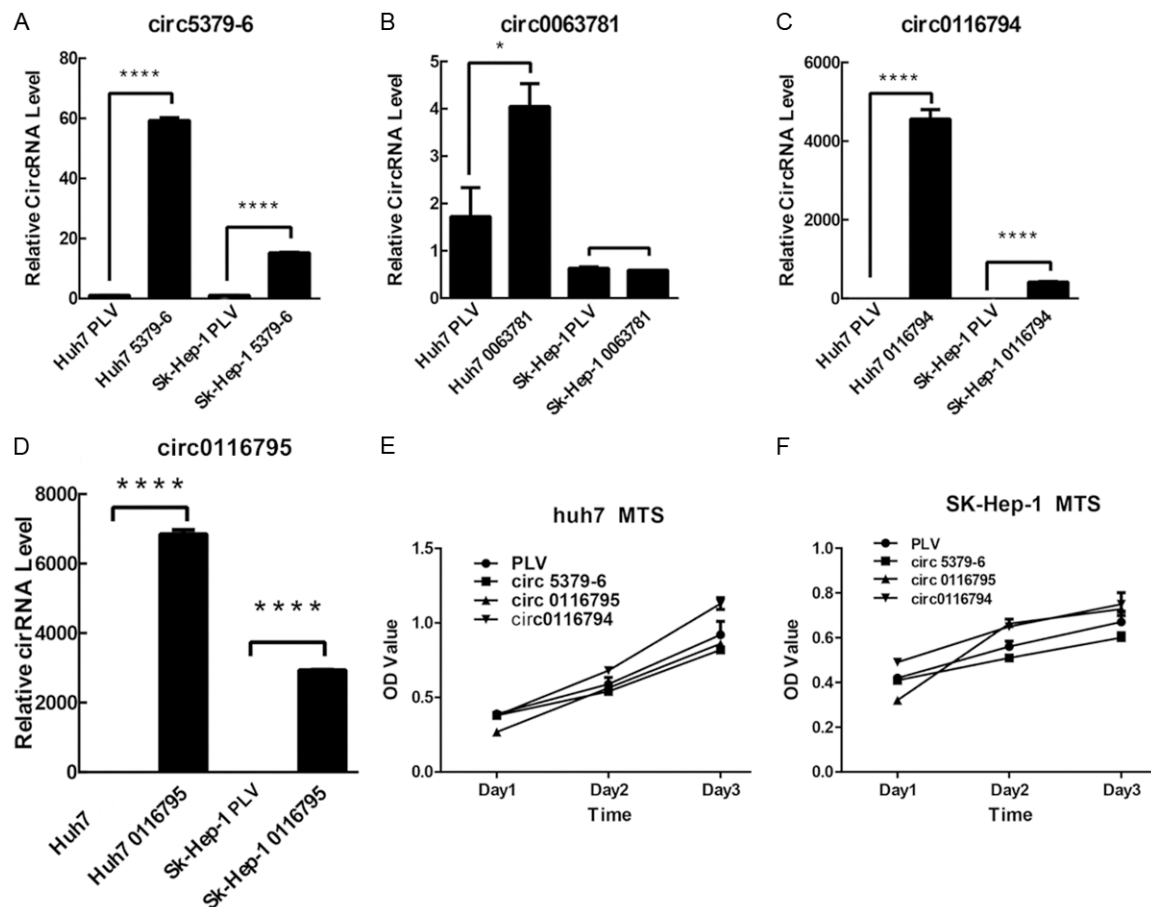


**Figure 3.** Validation the capacity of cell viability in hep-1 and huh7 cells. The performance of the overexpression vector of circ5379-6 (A), circ0063781 (B), circ0116794 (C), and circ0116795 (D) in hep-1 and huh7 cells. Circ5379-6 circ0116794 and circ0116795 were successfully overexpressed both in hep-1 and huh7 cells, then MTS assay were performed to detected the cell viability when they were overexpressed in huh7 (E) and hep-1 (F) cells. \*P<0.05; \*\*\*\*P<0.0001.

overexpression significantly suppressed the cell ability of both Huh-7 and Sk-hep-1 cells.

These findings allowed us to focus our functional analysis on circ5379-6 (Figure 3E and 3F).



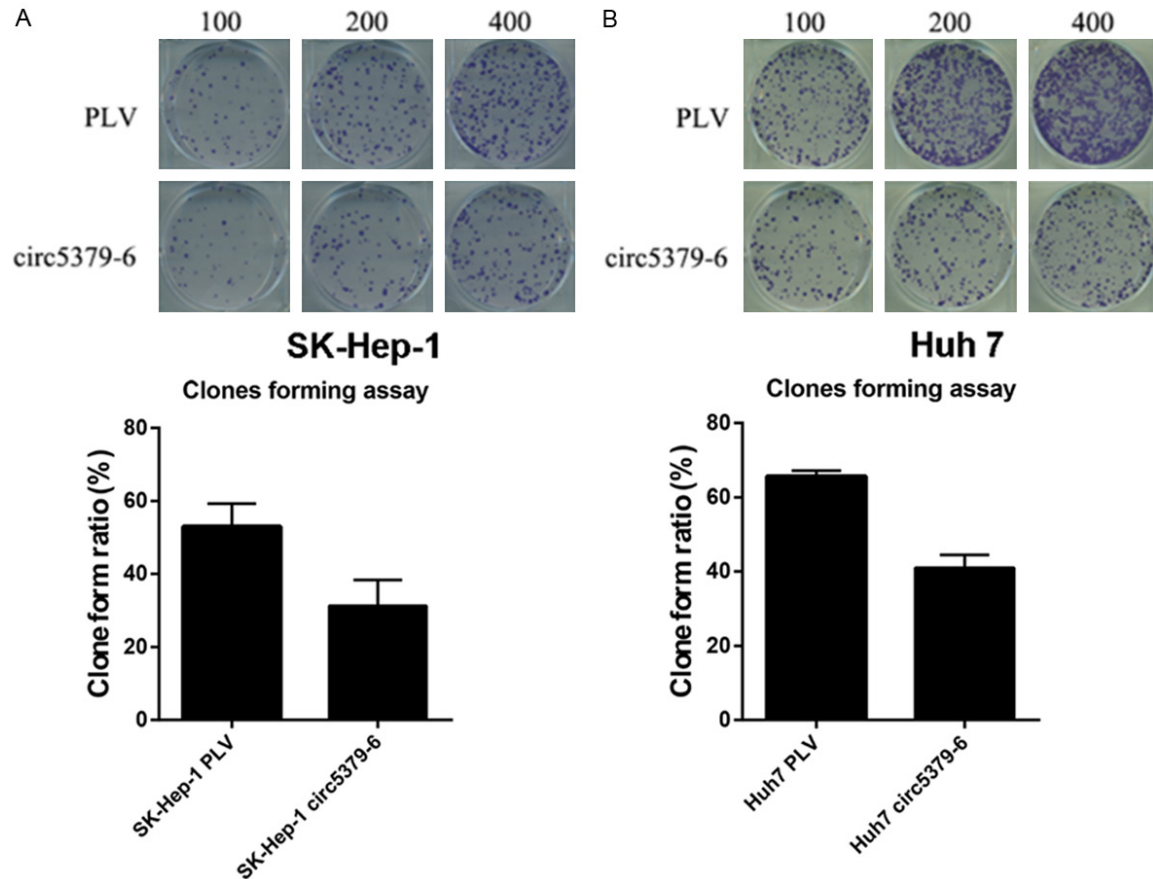


**Figure 4.** Overexpression of circ5379-6 and the corresponding effect on the cell colony formation. The overexpressed circ5379-6 induced the decreased numbers of cell colonies in hep-1 (A) and huh7 (B) cells.

*Circ5379-6 suppresses cell proliferation and metastasis in hepatocellular carcinoma cells*

To further investigate the functions of circ5379-6, a series of assays was conducted focusing on cell proliferation, migration and invasion, and the cell cycle. For the cell proliferation analysis, a cell colony assay was performed wherein different amounts of cells with/without circ5379-6 overexpression treatment were seeded on a 6-well plate and the cell colonies were counted after 2 weeks. The results were obvious that the overexpression of circ5379-6 decreased the number of cell colonies by 50% for both hep-1 and huh7 cell lines (**Figure 4A, 4B**). On the other hand, we detected the cell migration and cell invasion capacity using transwell assays. The cells that migrated to and invaded the bottom chamber were stained and counted. The migrated cell amounts were shown to be ~30% less and the invasive cell amounts were ~50% less in both cell lines after being subjected to overexpressed circ5379-6

(**Figure 5A, 5B**). The cells were further examined by flow cytometry. In the cell apoptosis assay, the percentages of cells in different states were measured. The most obvious effect of circ5379-6 was predicted to be the induction of cell apoptosis; the cell apoptosis percentage was significantly increased in accordance with an increased level of circ5379-6 (**Figure 6A**). However, in the cell cycle study, neither cell line showed a significant change in any phase, regardless of whether circ5379-6 was overexpressed or not (**Figure 6B**). Therefore, from the *in vitro* assays on the huh7 and hep-1 cell lines, circ5379-6 was shown to inhibit cell proliferation, migration, and invasion. It induced cell apoptosis by a mechanism other than regulation of the cell cycle.

*Circ5379-6 inhibits oncogenesis and metastasis in nude mice*

To confirm the observed effect of *Circ5379-6*, *in vivo* animal assays were performed in nude

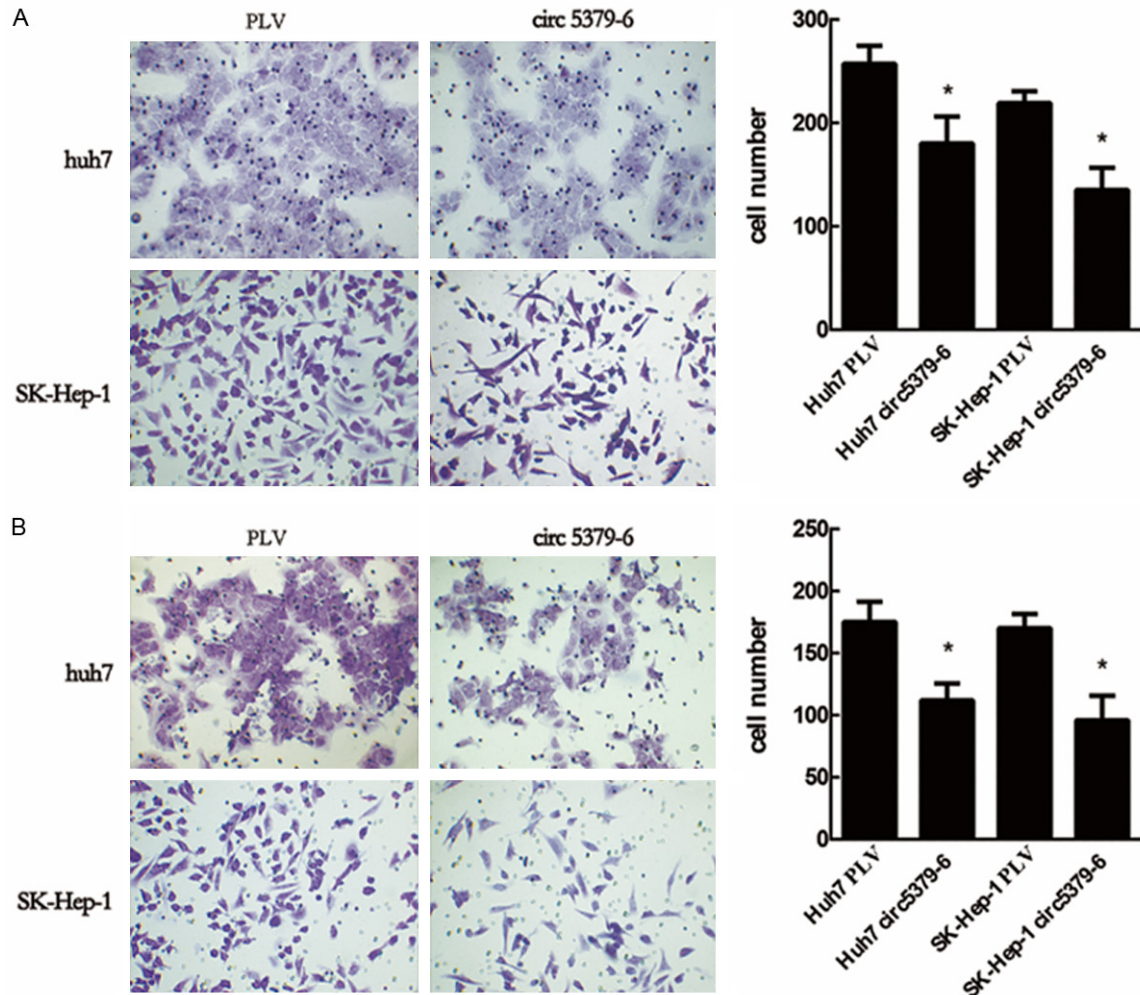


**Figure 5.** The functions of circ5379-6 on cell migration and invasion. A. Cell migration was affected by overexpressed circ5379-6, in which the migrated cells were accordingly decreased in huh7 and hep-1 cells; B. Cell invasion was inhibited by the overexpression of circ5379-6 in huh7 and hep-1 cells. \*P<0.05.

mice. Subcutaneous injection of the huh7 cells was performed for tumor generation. The size and weight of the tumor were measured (**Figure 7A**). The results clearly demonstrate that circ5379-6 performed inhibitory functions on the pathogenic process of hepatocellular carcinoma, as well in the *in vivo* condition. The size of the tumor gradually increased, but the development was inhibited in a positive correlation with the level of circ5379-6. Therefore, the size and weight of the tumor were smaller than those of the control group after overexpressing circ5379-6. According to the HE staining and immuno-histochemical staining, the features of the tumors are presented (**Figure 7B**). In the morphological analysis by HE staining, the tumorigenesis of the cells were inhibited with circ5379-6 treatment compared with the con-

trol group. However, the immuno-histochemical staining results show that cell migration and invasion related genes were differentially expressed in the experimental group. As seen in **Figure 7C**, MMP-9, Vimentin, and N-cadherin were all downregulated, while E-cadherin was upregulated in the tumor generated by the cells with circ5379-6 overexpression.

## Discussion

Currently, knowledge of the functions of circRNAs involved in HCC pathology is limited. Previous studies have shown that the downregulation of circ\_0001649 is related to HCC tumor size and tumor embolism. The downregulation of circ\_0004018 in HCC is associated with the serum alpha-fetoprotein level, tumor

# Circ5379-6 inhibits the tumorigenesis and metastasis of HCC

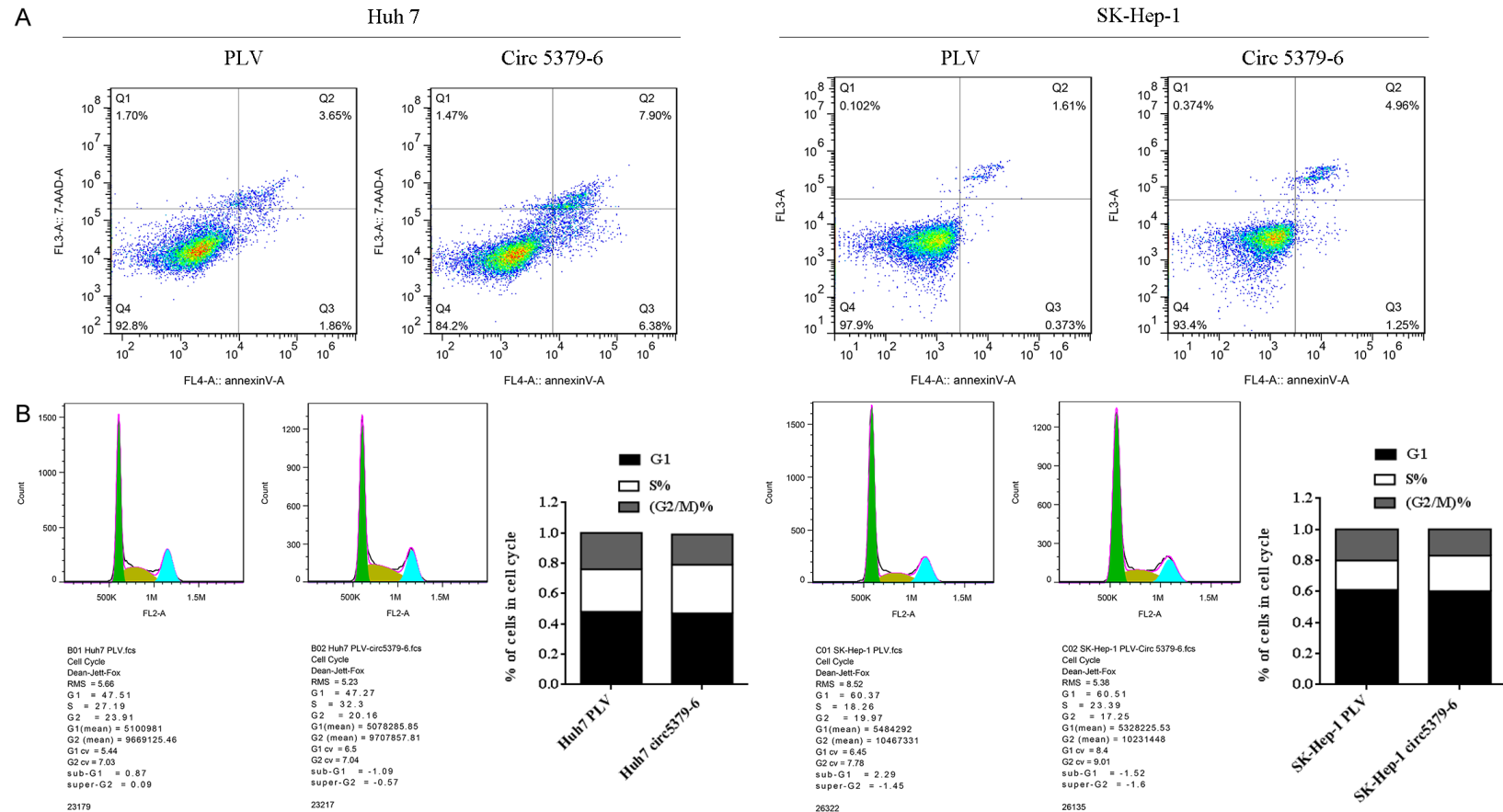


**Figure 6.** The functions of circ5379-6 on the cell cycle and apoptosis. A. Apoptosis was induced when circ5379-6 was overexpressed in huh7 and hep-1 cells; B. Overexpressed circ5379-6 did not obviously affect the S phase, or shorten the G2 phase in huh7 and hep-1 cells.



## Circ5379-6 inhibits the tumorigenesis and metastasis of HCC

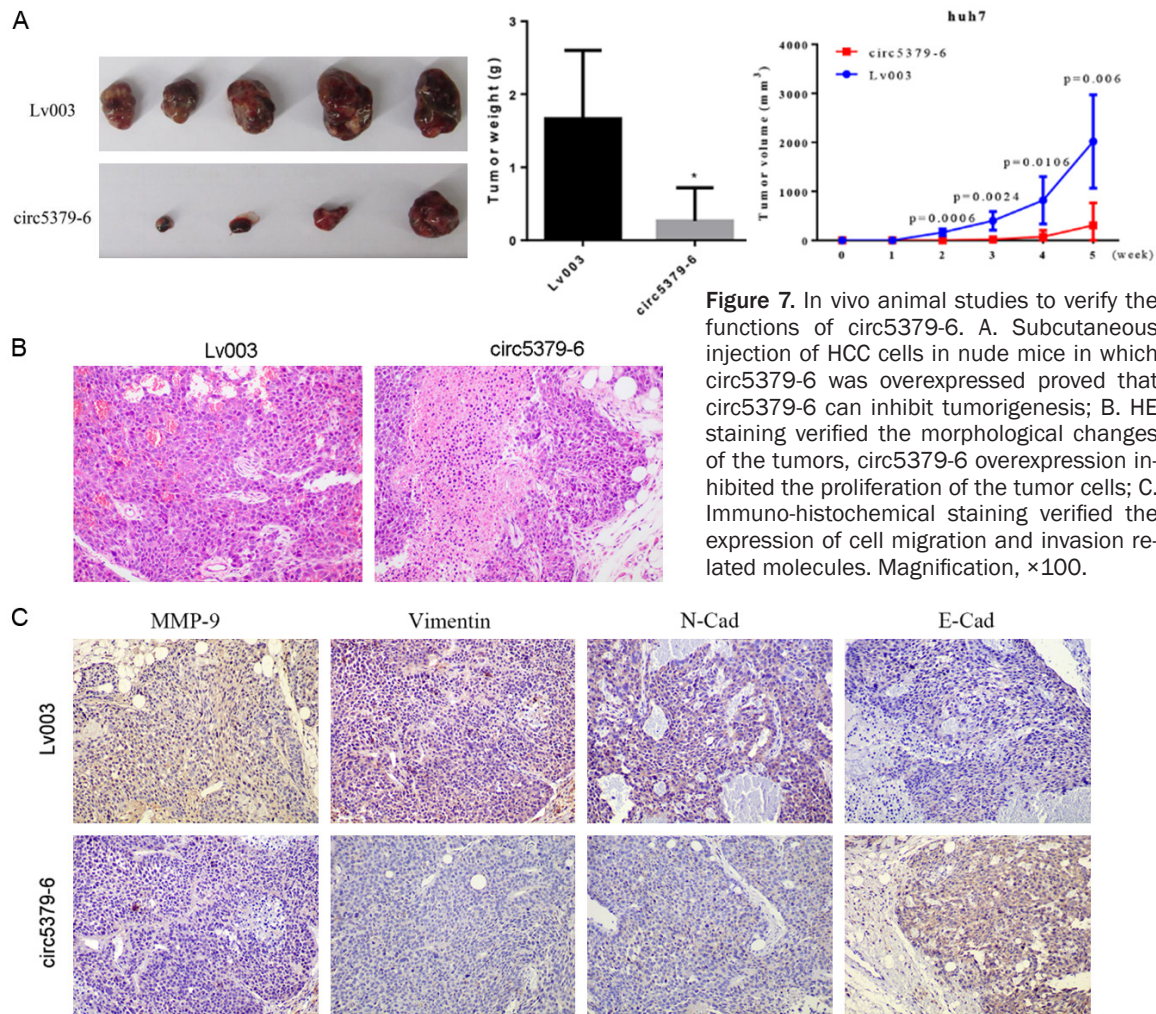


**Figure 7.** In vivo animal studies to verify the functions of circ5379-6. A. Subcutaneous injection of HCC cells in nude mice in which circ5379-6 was overexpressed proved that circ5379-6 can inhibit tumorigenesis; B. HE staining verified the morphological changes of the tumors, circ5379-6 overexpression inhibited the proliferation of the tumor cells; C. Immuno-histochemical staining verified the expression of cell migration and invasion related molecules. Magnification,  $\times 100$ .

diameter, differentiation, Barcelona clinical stage, and tumor lymph node metastasis, while upregulation of hsa\_circ\_0005075 and circ\_0004018 is closely related to tumor progression and can be used as potential biomarkers for liver cancer screening, treatment, and prognosis [12, 22, 23]. The famous miR-7 sponge, circular cdr1 (also known as ciRS-7) also plays a role in the promotion of HCC progression [24]. Han, *et al.*, found that circMTO1 can be used as a miR-9 sponge to regulate downstream p21 expression and inhibit the progression of liver cancer [25]. Yao, *et al.*, found that circZKSCAN1 and its corresponding linear mRNA seem to have the same effect on HCC growth, migration, and invasion, but through different signaling pathways, suggesting a relatively independent regulatory role of circRNA compared to its linear parent gene [21]. In this study, we extended the knowledge of circRNA function in HCC, showing that circ-5379-6 inhibited HCC growth and metastasis.

Although the role of circ-5379-6 has not been identified until now, its linear counterpart PPAR $\alpha$  gene has been reported to play an important role in suppressing malignant tumor progression and preventing carcinogenesis of kidney [26], breast [27], pancreatic [28], and colon cancers [29]. Our previous study also provided evidence for its inhibitory effect on HCC via the NF- $\kappa$ B signaling pathway [30]. In the present study, we suggested that the circular transcript product derived from PPAR $\alpha$  also exerted a similar effect on HCC progression. We identified 7 circRNAs derived from PPAR $\alpha$  mRNA for the first time and revealed the role of circ-5379-6 in inhibiting tumor growth and metastasis, both *in vitro* and *in vivo*. We excluded circ0116792, circ\_4706, and circ\_overlap-8 in this study for further function analyses, due to failed overexpression in both 293T and HepG2 cells. In addition, although we observed negative results on cell viability in circ63781, circ0116794, and circ0116795 overexpressed

cells and did not further analyze their effects on cell motility, we could not conclude that they have no function in HCC tumor metastasis. Therefore, whether or not these circRNAs have similar functions as their parent gene, *PPARα*, or with circ-5379-6, remains to be investigated in the future.

In addition to the findings on the inhibitory effect of circ-5379-6 in HCC tumor progression, a downregulation of MMP-9, Vimentin, and N-cadherin and an upregulation of E-cadherin were observed in the tumors of circ5379-6 overexpressing mice. Tumor metastasis is a complicated process. Of the involved steps, the degradation of the basement membrane and extracellular matrix is considered to be one of the most pivotal. Matrix metalloproteinase 9 (MMP-9) is a member of a family of zinc-dependent endopeptidases that function as metastasis promoters by destructing the extracellular matrix and degrading basement membranes during the metastasis process [31]. It is widely expressed in hepatocellular carcinoma during HCC metastasis and is usually in an activated state [32, 33]. The downregulation of MMP-9 has been observed in the reversal of liver cancer metastasis [34]. Epithelial-mesenchymal transition (EMT) is the process by which a cell gradually loses its epithelial phenotype, transforms into a mesenchymal phenotype, and experiences enhanced cell motility. E-cadherin is the most important epithelial molecular marker in EMT and also plays an important role in the process of tumor metastasis [35]. In the current study, downregulated MMP-9, Vimentin, and N-cadherin and upregulated E-cadherin were observed to partially reverse the EMT process and cell motility was suppressed, which may contribute to the inhibition of cell migration and invasion.

In conclusion, we found that a circular form of *PPARα*, a tumor suppressor, plays a role in the inhibition of tumor progression, similar to its corresponding linear *PPARα*.

## Acknowledgements

This research was supported by National Nature Science Foundation of China (81401999, 81630018, 81870384, 81772635), and Nature Science Foundation of Guangdong (2014-A030313208).

## Disclosure of conflict of interest

None.

**Address correspondence to:** Dr. Minhu Chen, Department of Gastroenterology, The First Affiliated Hospital, Sun Yat-sen University, No. 58 Zhongshan II Road, Guangzhou 510080, China. Tel: +86-020-87755766; Fax: +86-020-87755766; E-mail: chen-minhu@mail.sysu.edu.cn

## References

- [1] El-Serag HB and Rudolph KL. Hepatocellular carcinoma: epidemiology and molecular carcinogenesis. *Gastroenterology* 2007; 132: 2557-2576.
- [2] Zhao H, Zou LW and Zheng SS. Association between the NQO1 C609T polymorphism with hepatocellular carcinoma risk in the Chinese population. *Asian Pac J Cancer Prev* 2015; 16: 1821-1825.
- [3] Parkin DM. Global cancer statistics in the year 2000. *Lancet Oncol* 2001; 2: 533-543.
- [4] Yuen MF, Hou JL, Chutaputti A; Asia Pacific Working Party on Prevention of Hepatocellular Carcinoma. Hepatocellular carcinoma in the Asia pacific region. *J Gastroenterol Hepatol* 2009; 24: 346-353.
- [5] Chen LL. The biogenesis and emerging roles of circular RNAs. *Nat Rev Mol Cell Biol* 2016; 17: 205-211.
- [6] Guo JU, Agarwal V, Guo H and Bartel DP. Expanded identification and characterization of mammalian circular RNAs. *Genome Biol* 2014; 15: 409.
- [7] Li F, Zhang L, Li W, Deng J, Zheng J, An M, Lu J and Zhou Y. Circular RNA ITCH has inhibitory effect on ESCC by suppressing the Wnt/beta-catenin pathway. *Oncotarget* 2015; 6: 6001-6013.
- [8] Jeck WR, Sorrentino JA, Wang K, Slevin MK, Burd CE, Liu J, Marzluff WF and Sharpless NE. Circular RNAs are abundant, conserved, and associated with ALU repeats. *Rna* 2013; 19: 141-157.
- [9] Schwanhauser B, Busse D, Li N, Dittmar G, Schuchhardt J, Wolf J, Chen W and Selbach M. Global quantification of mammalian gene expression control. *Nature* 2011; 473: 337-342.
- [10] Hansen TB, Jensen TI, Clausen BH, Bramsen JB, Finsen B, Damgaard CK and Kjems J. Natural RNA circles function as efficient microRNA sponges. *Nature* 2013; 495: 384-388.
- [11] Hansen TB, Kjems J and Damgaard CK. Circular RNA and miR-7 in cancer. *Cancer Res* 2013; 73: 5609-5612.
- [12] Qin M, Liu G, Huo X, Tao X, Sun X, Ge Z, Yang J, Fan J, Liu L and Qin W. Hsa\_circ\_0001649: a circular RNA and potential novel biomarker for hepatocellular carcinoma. *Cancer Biomark* 2016; 16: 161-169.
- [13] Huang XY, Huang ZL, Xu YH, Zheng Q, Chen Z, Song W, Zhou J, Tang ZY and Huang XY. Com-

- prehensive circular RNA profiling reveals the regulatory role of the circRNA-100338/miR-141-3p pathway in hepatitis B-related hepatocellular carcinoma. *Sci Rep* 2017; 7: 5428.
- [14] Shi L, Yan P, Liang Y, Sun Y, Shen J, Zhou S, Lin H, Liang X and Cai X. Circular RNA expression is suppressed by androgen receptor (AR)-regulated adenosine deaminase that acts on RNA (ADAR1) in human hepatocellular carcinoma. *Cell Death Dis* 2017; 8: e3171.
- [15] Desvergne B and Wahli W. Peroxisome proliferator-activated receptors: nuclear control of metabolism. *Endocr Rev* 1999; 20: 649-688.
- [16] Li G, Bocker CN, Yan T, Xie C, Krausz KW, Xiang R and Gonzalez FJ. Metabolic adaptation to intermittent fasting is independent of peroxisome proliferator-activated receptor alpha. *Mol Metab* 2018; 7: 80-89.
- [17] Yeldandi AV, Rao MS and Reddy JK. Hydrogen peroxide generation in peroxisome proliferator-induced oncogenesis. *Mutat Res* 2000; 448: 159-177.
- [18] Misra P and Reddy JK. Peroxisome proliferator-activated receptor-alpha activation and excess energy burning in hepatocarcinogenesis. *Biochimie* 2014; 98: 63-74.
- [19] Gonzalez FJ, Peters JM and Cattley RC. Mechanism of action of the nongenotoxic peroxisome proliferators: role of the peroxisome proliferator-activator receptor alpha. *J Natl Cancer Inst* 1998; 90: 1702-1709.
- [20] Zhang N, Chu ES, Zhang J, Li X, Liang Q, Chen J, Chen M, Teoh N, Farrell G, Sung JJ and Yu J. Peroxisome proliferator activated receptor alpha inhibits hepatocarcinogenesis through mediating NF-kappaB signaling pathway. *Oncotarget* 2014; 5: 8330-8340.
- [21] Yao Z, Luo J, Hu K, Lin J, Huang H, Wang Q, Zhang P, Xiong Z, He C, Huang Z, Liu B and Yang Y. ZKSCAN1 gene and its related circular RNA (circZKSCAN1) both inhibit hepatocellular carcinoma cell growth, migration, and invasion but through different signaling pathways. *Mol Oncol* 2017; 11: 422-437.
- [22] Shang X, Li G, Liu H, Li T, Liu J, Zhao Q and Wang C. Comprehensive circular RNA profiling reveals that hsa\_circ\_0005075, a new circular RNA biomarker, is involved in hepatocellular carcinoma development. *Medicine (Baltimore)* 2016; 95: e3811.
- [23] Fu L, Yao T, Chen Q, Mo X, Hu Y and Guo J. Screening differential circular RNA expression profiles reveals hsa\_circ\_0004018 is associated with hepatocellular carcinoma. *Oncotarget* 2017; 8: 58405-58416.
- [24] Yu L, Gong X, Sun L, Zhou Q, Lu B and Zhu L. The circular RNA Cdr1as act as an oncogene in hepatocellular carcinoma through targeting miR-7 expression. *PLoS One* 2016; 11: e0158347.
- [25] Han D, Li J, Wang H, Su X, Hou J, Gu Y, Qian C, Lin Y, Liu X, Huang M, Li N, Zhou W, Yu Y and Cao X. Circular RNA circMTO1 acts as the sponge of microRNA-9 to suppress hepatocellular carcinoma progression. *Hepatology* 2017; 66: 1151-1164.
- [26] Abu Aboud O, Wettersten HI and Weiss RH. Inhibition of PPARalpha induces cell cycle arrest and apoptosis, and synergizes with glycolysis inhibition in kidney cancer cells. *PLoS One* 2013; 8: e71115.
- [27] Bocca C, Bozzo F, Martinasso G, Canuto RA and Miglietta A. Involvement of PPARalpha in the growth inhibitory effect of arachidonic acid on breast cancer cells. *Br J Nutr* 2008; 100: 739-750.
- [28] Xue J, Zhu W, Song J, Jiao Y, Luo J, Yu C, Zhou J, Wu J, Chen M, Ding WQ, Cao J and Zhang S. Activation of PPARalpha by clofibrate sensitizes pancreatic cancer cells to radiation through the Wnt/beta-catenin pathway. *Oncogene* 2018; 37: 953-962.
- [29] Jackson L, Wahli W, Michalik L, Watson SA, Morris T, Anderton K, Bell DR, Smith JA, Hawkey CJ and Bennett AJ. Potential role for peroxisome proliferator activated receptor (PPAR) in preventing colon cancer. *Gut* 2003; 52: 1317-1322.
- [30] Zhang N, Chu ES, Zhang J, Li X, Liang Q, Chen J, Chen M, Teoh N, Farrell G, Sung JJ and Yu J. Peroxisome proliferator activated receptor alpha inhibits hepatocarcinogenesis through mediating NF-kappaB signaling pathway. *Oncotarget* 2014; 5: 8330-8340.
- [31] John A and Tuszynski G. The role of matrix metalloproteinases in tumor angiogenesis and tumor metastasis. *Pathol Oncol Res* 2001; 7: 14-23.
- [32] Zhang Y, Shen Y, Cao B, Yan A and Ji H. Elevated expression levels of androgen receptors and matrix metalloproteinase-2 and -9 in 30 cases of hepatocellular carcinoma compared with adjacent tissues as predictors of cancer invasion and staging. *Exp Ther Med* 2015; 9: 905-908.
- [33] Chen JS, Huang XH, Wang Q, Huang JQ, Zhang LJ, Chen XL, Lei J and Cheng ZX. Sonic hedgehog signaling pathway induces cell migration and invasion through focal adhesion kinase/AKT signaling-mediated activation of matrix metalloproteinase (MMP)-2 and MMP-9 in liver cancer. *Carcinogenesis* 2013; 34: 10-19.
- [34] Liu J, Wen X, Liu B, Zhang Q, Zhang J, Miao H and Zhu R. Diosmetin inhibits the metastasis of hepatocellular carcinoma cells by downregulating the expression levels of MMP-2 and MMP-9. *Mol Med Rep* 2016; 13: 2401-2408.
- [35] Mittal V. Epithelial mesenchymal transition in tumor metastasis. *Annu Rev Pathol* 2018; 13: 395-412.



# Circ5379-6 inhibits the tumorigenesis and metastasis of HCC

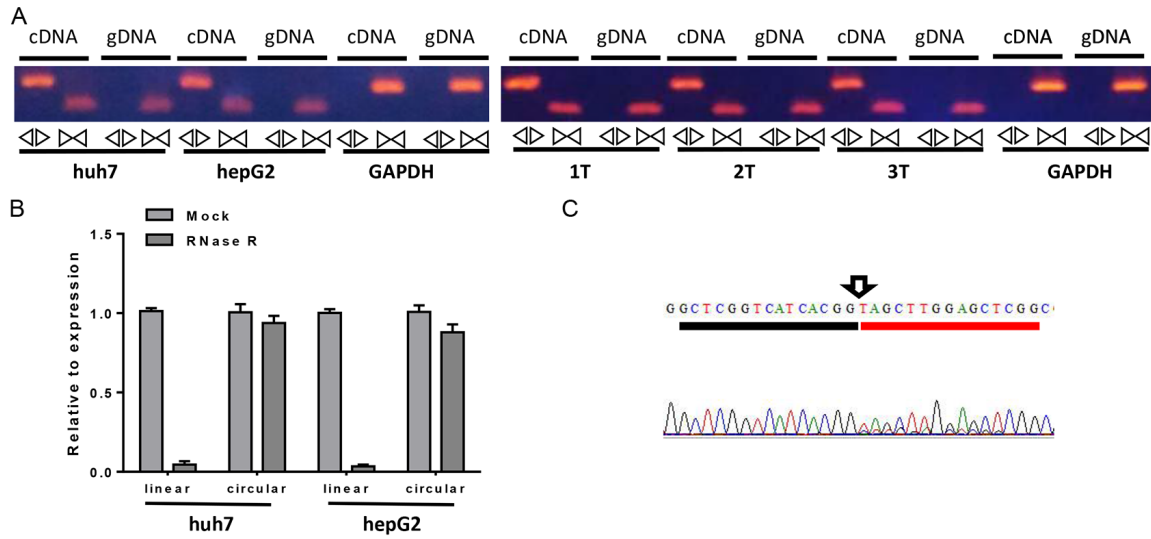


**Figure S1.** Verification the Cyclization sites and Characterization of has\_circ\_0063781. A. Divergent primers amplify circular RNAs in cDNA but not genomic DNA (gDNA) in huh7, hepG2 cell lines and hepatocarcinoma tissues. Convergent primers can amplify both circular RNAs and liner RNAs, GAPDH, liner control. B. The predicted circular RNA is resistant to RNase R treatment. C. Sequencing depicts the junction of hsa\_circ\_0063781.

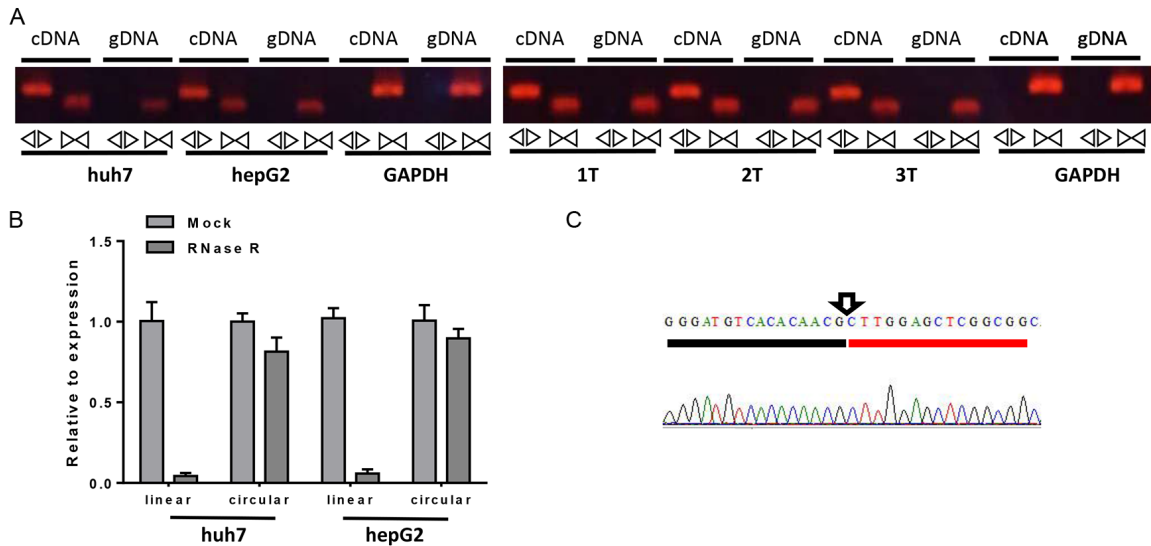


**Figure S2.** Verification the Cyclization sites and Characterization of hsa\_circ\_0116792. A. Divergent primers amplify circular RNAs in cDNA but not genomic DNA (gDNA) in huh7, hepG2 cell lines and hepatocarcinoma tissues. Convergent primers can amplify both circular RNAs and liner RNAs, GAPDH, liner control. B. The predicted circular RNA is resistant to RNase R treatment. C. Sequencing depicts the junction of hsa\_circ\_0116792.



## Circ5379-6 inhibits the tumorigenesis and metastasis of HCC

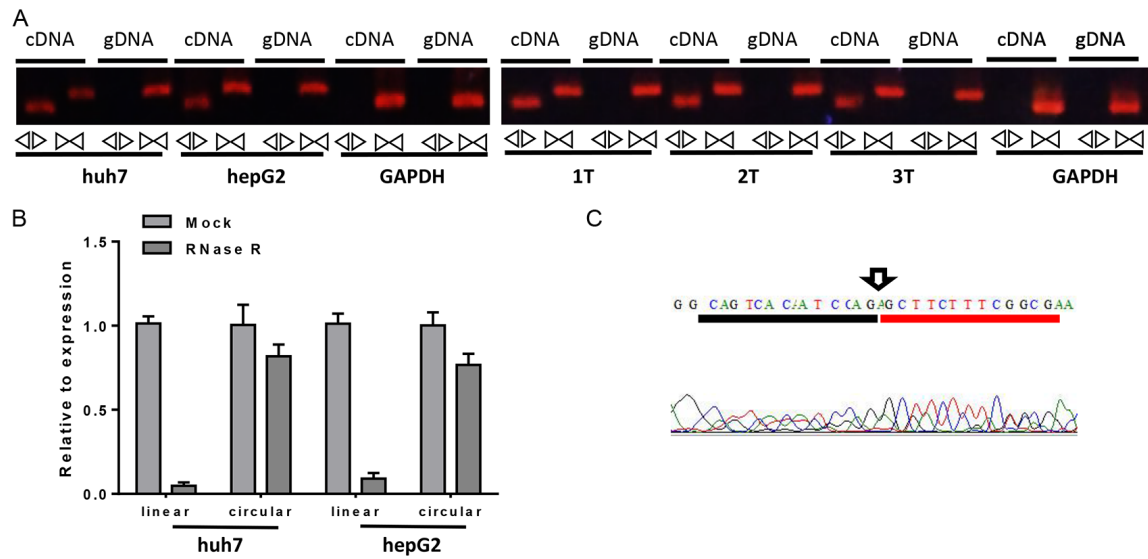


**Figure S3.** Verification the Cyclization sites and Characterization of hsa\_circ\_0116794. A. Divergent primers amplify circular RNAs in cDNA but genomic DNA (gDNA) in huh7, hepG2 cell lines and hepatocarcinoma tissues. Convergent primers can amplify both circular RNAs, GAPDH, linear control. B. The predicted circular RNA is resistant to RNase R treatment. C. Sequencing depicts the junction of hsa\_circ-0116794.

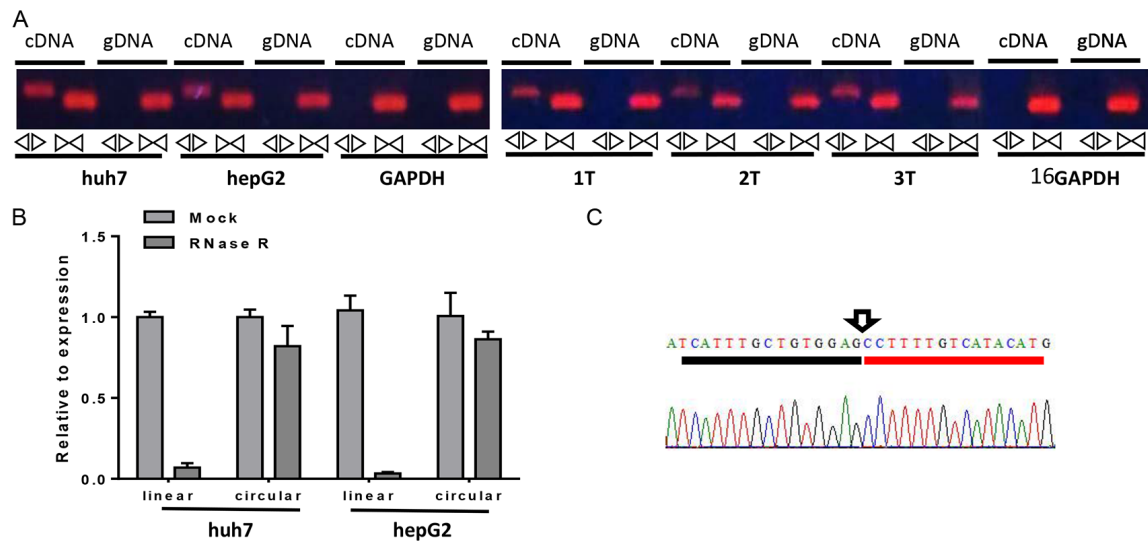


**Figure S4.** Verification the cyclization sites and characterization of hsa\_circ\_0116795. A. Divergent primers amplify circular RNAs in cDNA but not genomic DNA (gDNA) in huh7, hepG2 cell lines and hepatocarcinoma tissues. Convergent primers can amplify both circular RNAs and linear RNAs, GAPDH, linear control. B. The predicted circular RNA is resistant to RNase R treatment. C. Sequencing depicts the junction of hsa\_circ\_0116795.

## Circ5379-6 inhibits the tumorigenesis and metastasis of HCC

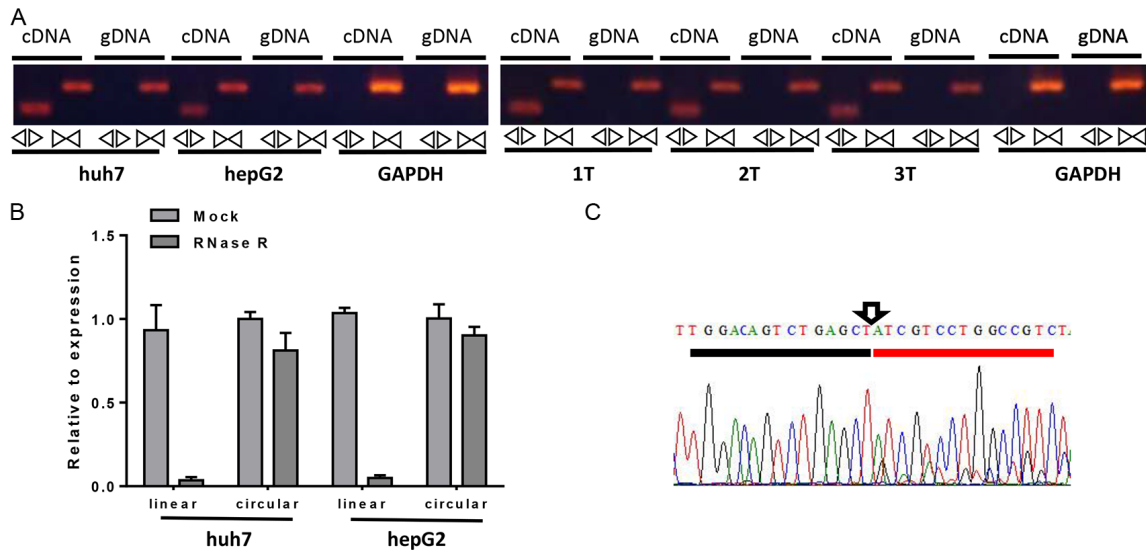


**Figure S5.** Verification the Cyclization sites and Characterization of hsa\_circ\_0004706. A. Divergent primers amplify RNAs in cDNA but not genomic DNA (gDNA) in huh7, hepG2, linear control. B. The predicted circular RNA is resistant to RNase R treatment. C. Sequencing depicts the junction of hsa\_circ\_0004706.

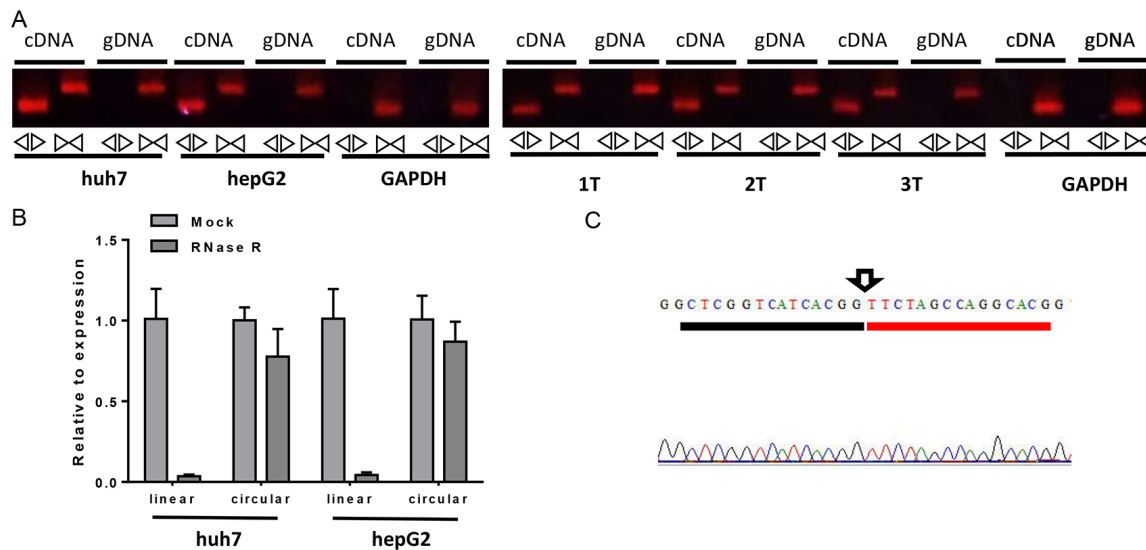


**Figure S6.** Verification the cyclization sites and characterization of hsa\_circ\_PPARG-overlap-8. A. Divergent primers amplify circular RNAs in cDNA but not genomic DNA (gDNA) in huh7, hepG2, cell lines and hepatocarcinoma tissues. Convergent primers can amplify both circular RNAs and RNAs, GAPDH, linear control. B. The predicted circular RNA is resistant to RNase R treatment. C. Sequencing depicts the junction of hsa\_circ\_PPARG-overlap-8.